Alkali-silica reaction (ASR) expansion: Pessimum effect versus scale effect

Xiao Xiao Gao, Stéphane Multon, Martin Cyr, Alain Sellier

Alkali-silica reaction (ASR) expansion: pessimum effect versus scale effect

Xiao Xiao Gao [a], Stéphane Multon [a*], Martin Cyr [a], Alain Sellier [a]

[(a)] *Université de Toulouse; UPS, INSA; LMDC (Laboratoire Matériaux et Durabilité des Constructions); 135, avenue de Rangueil; F-31 077 Toulouse Cedex 04, France*

Abstract

The effect of aggregate size on ASR expansions has been largely studied and conflicting results exist concerning the aggregate size that leads to the highest ASR expansion. Most of the research works clearly show a pessimum effect of aggregate size on ASR expansion. However, all the results available in the literature were obtained using different experimental conditions and the combined effects of other important parameters, such as specimen size used in the expansion tests, have often been neglected. This paper aims to investigate the combined effect of specimen size and aggregate size on ASR expansion. Experimental results highlight a scale effect, a combination of the effects of aggregate size and specimen size on ASR expansion. This scale effect appears to be influenced by the reactive silica content of the aggregate. Modelling at microscopic level is used to propose a quantification of this effect.

Keywords: alkali-silica reaction (ASR), particle size, specimen size, expansion, scale effect

[*] Corresponding author. *e-mail address:* multon@insa-toulouse.fr (Stéphane Multon)

1. Introduction

Alkali-Silica Reaction (ASR) is a deleterious chemical reaction occurring in all types of structures that contain alkali-reactive aggregates: dams, bridges, roads, breakwaters, etc. The mechanism of expansion can be described in three main steps [1-4]: the diffusion of ionic species (Na^+, K^+, OH^-, Ca^{2+}) into the aggregates, the disruption of the silanol and siloxane bonds contained in the reactive silicate, and the reaction of alkali silicate with ionic species (Na^+, K^+, Ca^{2+}) to form ASR gels. ASR gel induces pressure in the aggregate and in the cement paste, leading to stresses and thus cracking. ASR expansion depends on numerous parameters (amounts of alkali, reactive silica and water present, aggregate and specimen sizes, etc.).

It seems that the range of aggregate size causing the highest ASR expansion varies with the nature and composition of the aggregate. Numerous papers [5-23] discuss the effect on ASR expansion of particle sizes of reactive aggregates like opal [5-12], various kinds of silica glass, fused silica and waste silica glass, and so on [13-24]. Some research has shown that the expansion induced by ASR increases as the reactive particle size is reduced [9,14,17,19]. Some authors obtained insignificant expansion when the sizes of the reactive particles were under 50 to 150 µm [11,13,15,22]. Furthermore, the use of powder from reactive aggregates like pozzolans, with particle sizes up to about 100 µm, has been developed to counteract the effect of ASR [15,18,21]. Only a few exceptions with very small particles led to significant ASR expansions, all involving opal aggregates [5-7, 12]. Other research works have shown a pessimum effect for various types of aggregates, with pessimum values occurring in a wide interval of particle sizes [4,7,8,10-13,16,20,23,24]. It is observed that, in some cases, the most damaging size, leading to the highest ASR expansion, reaches more than 1 mm. The effect of "specimen size" has been much less studied [25-28]. Experiments performed with different

51 ‘aggregate size to specimen size’ ratios show the effect of the size of the specimens on the
52 ASR expansions measured. Lower expansions were measured on the smaller specimens
53 [25,26].
54 First, a literature review showed that conflicting results exist concerning the most damaging
55 reactive aggregate size, which leads to the highest ASR expansion. Secondly, experimentation
56 performed by Zhang et al. [26] suggested that the two effects of aggregate and specimen sizes
57 are combined. Therefore, the difficulty in generalizing results on the effect of the particle size
58 of reactive aggregates could be explained by the differences in experimental conditions, and
59 particularly the combined effects of aggregate size and specimen size on ASR expansion. This
60 paper aims to investigate and quantify this scale effect and the influence the reactive silica
61 content of aggregate has on the effect, in order to gain a better understanding of expansion
62 tests.
63 The development of an ASR model at the microscopic level is a major concern of researchers
64 trying to understand the mechanisms involved in the ASR and to predict future expansion.
65 Previous modelling investigated the different aspects of the reaction: the mechanical
66 consequences of ASR [29-32], the chemical mechanisms driving the attack of the aggregate
67 by hydroxyl ions [33] and their coupling [34-38]. These works do not take into account the
68 permeation of ASR gels in cracks which could be the main cause of the decrease of expansion
69 by pessimum or scale effects. The concepts of fracture mechanics can explain the cracking
70 phenomenon in the cases of aggregate in infinite matrix [39, 40] or of central penny-shaped
71 crack in sphere [41]. However, it is difficult to apply such models in the cases of specimens
72 containing aggregates with numerous interactions (interactions with other neighbour
73 aggregates and with specimen boundaries). The experiments presented in this paper were used
74 to point out the dependence of expansion with aggregate and specimen sizes. These results are
75 explained by fracture mechanics concepts. The teachings pointed out by fracture mechanics

are then used to propose a simplified relationship to take into account the scale effect in an analytical modelling. Finally, the experimental results are used here to calibrate and discuss the validity and the capability of the model.

2. Experimental conditions and results

2.1 Experimental conditions

Expansion was measured on mortar prisms with a water/cement ratio of 0.5 and a sand (1512 kg/m^3) / cement (504 kg/m^3) ratio of 3. Mixtures were adjusted by adding NaOH to the mixing water in order to have the same alkali concentration in the pore solution and in the storage solution. For the reference specimens, the sand was composed of the non-reactive marble only. For all the other specimens, the sand contained 30% of reactive aggregate and 70% of non-reactive marble. The prisms were stored in NaOH solution at 60°C. The expansion measurements were performed after the prisms had cooled to 20ºC (~12 h) in the NaOH solution. Each variation of length value was calculated as the mean of three values from three replicate specimens measured using the scale micrometer method (specimens had shrinkage bolts in the two extremities) [42,43]. The experimentation presented in this paper aimed to study three particular points:

Effect of alkali concentration

As explained above, the specimens were kept immersed in NaOH solution. The aim of this part was to study three NaOH concentrations for immersion close to the standard conditions of 1 mol/l (0.77, 1 and 1.25 mol/l). Reactive siliceous limestone was used to study the effect of alkali concentration on ASR expansion. The specimen and aggregate sizes were respectively 20 x 20 x 160 mm and 315-1250 µm (15% of 315-630 and 15% of 630-1250 µm). Eighteen specimens (nine reactive and nine reference specimens) were used for this part of the experimentation.

Effect of reactive silica content

The second point concerned the effect of the reactive aggregate nature on ASR expansion. Four reactive aggregates with different reactive silica contents were chosen and tested. Opal (O) is known to be very reactive and to give large expansion if the amount of available alkali is sufficient. Quartzite (Q) and siliceous limestone (SL) are usually less reactive but can exhibit significant expansion in concrete. Quartz aggregate (QA), which contains mostly quartz, is considered as non-reactive. The silica contents of the aggregate [43] are given in Table 1. The aggregates were used to cast 20x20x160 mm specimens with 315-1250 µm reactive aggregate (15% of 315-630 and 15% of 630-1250 µm). The fifteen specimens were kept in 1 mol/l NaOH solution.

Combined effect of aggregate and specimen sizes

Four reactive aggregate size classes: C1 (0-315 µm), C2 (315-630 µm), C3 (630-1250 µm) and C4 (1250-2500 µm) and three specimen sizes: 20x20x160 mm, 40x40x160 mm and 70x70x280 mm were used to research the combined effect of aggregate and specimen sizes on ASR expansion. The forty-five specimens (thirsty-six reactive and nine non-reactive specimens) were stored in 1 mol/l NaOH solution. Siliceous limestone was used as the reactive aggregate.

2.2 Experimental results

2.2.1 Effect of the alkali concentration

The final expansions for the three NaOH concentrations of 0.77, 1.0 and 1.25 mol/l were 0.67%, 0.64% and 0.60% respectively (Figure 1). The difference between two consecutive concentrations appeared to be small considering that the standard deviation for the specimens was in the range of 0~0.02%. Between 0.77 and 1.25 mol/l, the alkali concentrations could be considered to have little influence on ASR expansions in conditions of abundant alkali.

2.2.2 Effect of the reactive silica content

The ASR expansions obtained for the four aggregates are plotted in Figure 1. The specimens containing opal were the most reactive, with fast expansion and an asymptotic value of about 1.35%. The specimens with siliceous limestone exhibited rapid expansion, but the final expansions were lower (about 0.6%). The specimens with quartzite aggregate presented a slow expansion rate but reached a final expansion of about 0.55%. ASR expansion of the specimens containing quartz aggregate was about 0.14%. By the end of the experiment, the specimens containing opal were seriously damaged and cracked (crack width of about 425 µm) while the other specimens showed cracks with widths smaller than 10 µm (Figure 2). The reliability of measured expansions could have been affected by such cracking. However, the coefficient of variations obtained for three specimens was lower than 5%. It shows that the expansion scattering stayed quite small in spite of the large cracks.

2.2.3 Combined effects of aggregate and specimen sizes

The ASR expansions obtained for mortars containing the reactive siliceous limestone with various aggregate sizes and cast in specimens of different sizes are given in Figure 3. First, the specimens containing small reactive particles (0-315 µm) had the smallest expansion (lower than 0.15%), confirming results found in the literature. The ASR expansions were significant and higher than 0.5% for the other three aggregate sizes. Concerning final ASR expansion, the largest specimens showed the highest ASR expansion (Figure 4). This was particularly significant on the large aggregate class 1250-2500 µm (ASR expansions were twice as large for the 70x70x280-mm specimens as for the others). Moreover, ASR expansions presented a pessimum effect with the reactive aggregate size (with a final expansion larger for the aggregate size 315-630 µm than for 1200-2500 µm) for measurements performed on the smallest specimens (20x20x160 mm, 40x40x160 mm) but

149 not for the largest ones (Figure 4). These observations show the significant combined effect of
150 specimen size and aggregate size.

151 ### *2.2.4 Scale effect*

152 ***Mechanisms***

153 In order to understand the scale effect (combination of the aggregate- and specimen-size
154 effects on expansion), the ASR development can be described in four phases:

155 1. Ions (hydroxyls and alkalis) from the pore solution diffuse into the aggregates whatever the
156 reactive silica distribution in the aggregate (uniform or in veins – Figure 5-a).

157 2. Ions react with reactive silica and ASR gel is created in and/or around the aggregate
158 (according to the distribution of the reactive silica in the aggregate, a part of the reactive silica
159 can even be in direct contact with cement paste – Figure 5-b). A part of the gel can fill the
160 connected porous volume surrounding the aggregate without leading to damage [33-35,39]
161 (Figure 5-b) and also a part of the porosity of the aggregate close to the reactive site which
162 can lead to the cracking of veined aggregates [41]. This can explain why the smallest
163 aggregates lead to small expansion. For the same reactive silica content, more of the gel can
164 migrate in the connected porosity for the smallest aggregates than for larger aggregates. Thus,
165 a small amount of ASR gel is able to cause expansion [23,34,39]. It is easier for the cement
166 paste to accommodate ASR gel when the gel is created by a large number of small sites rather
167 than by a small number of scattered, larger sites.

168 3. ASR gel exerts pressures on the surrounding aggregate and cement paste when a part of the
169 connected porosity is filled (Figure 5-c) and the gel can no longer move in the porosity. In
170 order to assess the gel pressure p_g^a for the aggregate of size a, an analogy with previous
171 modelling [23, 34] can be made. In these works, the ASR mechanical effect was assumed to
172 be an imposed strain of the aggregate on the surrounding cement paste equal to:

$$\varepsilon_{imp}^{a} = \frac{\left\langle V_a^{gel} - V_a^{poro} \right\rangle^+}{V_a} \quad (1)$$

$\left\langle X \right\rangle^+$ is the positive part of X: if $X<0$, $\left\langle X \right\rangle^+ = 0$ otherwise $\left\langle X \right\rangle^+ = X$

V_a^{gel} is the volume of ASR gel formed in reactive aggregates and V_a, the volume of the reactive aggregate, $V_a = \frac{4}{3}\pi \cdot R_a^3$ (if spherical shape is assumed for aggregate).

V_a^{poro} is the volume of the porosity in which the ASR gel can migrate without causing expansion. It was assumed that the proportion of gels filling the porosity connected to the reactive sites (cement paste and aggregate) without creating pressure was the total volume of porosity filled by the gel with an equivalent thickness t_c, which was assumed to be independent of the aggregate size:

$$V_a^{poro} = \varphi \frac{4}{3}\pi \cdot \left((R_a + t_c)^3 - R_a^3 \right) \quad (2)$$

where φ is the porosity of the mortar. In reality, it includes a part of aggregate porosity but, by sake of simplicity, the model considers the thickness t_c as the average distance of gel penetration which should depend on the gel pressure: penetration is more or less difficult due to the ASR gel viscosity, its surface tension and the size of the pores of the aggregate and of the cement paste surrounding the reactive sites [39]. Once the gel reaches t_c, it cannot penetrate in the paste anymore due to the combination of these three main parameters. They were assumed to be the same for all the aggregates and that's why the equivalent thickness t_c was assumed to be independent with the aggregate size.

In order to assess the effect of ASR-gel on the cement paste in term of pressure, similar relationship can be used. p_g^a, the gel pressure can be assumed to be proportional to M_g the gel bulk modulus and to the increase of volume due to ASR-gel production:

$$p_g^a(t) = M_g \left\langle V_a^{gel} - \varphi \frac{4}{3}\pi \left[(R_a + t_c)^3 - R_a^3 \right] \right\rangle \quad (3)$$

192 V_a^{gel}, the volume of ASR gel formed in reactive aggregates, is proportional to the number of
193 moles of ASR gel formed after the attack of the reactive silica:

$$V_a^{gel} = n_a^{gel} \cdot V_{gel}^{mol} \tag{4}$$

194 with n_a^{gel} *(mol):* the number of moles of ASR gel produced by the aggregate *a* and V_{gel}^{mol}
195 *(m^3/mol):* the molar volume of the gel.
196 The number of moles of ASR gels produced by the reaction is defined by the number of
197 moles of silica attacked by alkalis and can be taken proportional to *s* the reactive silica content
198 (in mol/m^3):

$$n_a^{gel} = \frac{4}{3}\pi R_a^3 \cdot s \cdot \zeta(t) \tag{5}$$

199 $\zeta(t)$ is the chemical advancement of the alkali-silica reaction (which depends on temperature,
200 moisture and alkali conditions and is assessed by the diffusion of ionic species in the
201 aggregate and by the time necessary for the attack of the reactive silica by hydroxyl ions and
202 for the formation of ASR-gels [34]).
203 Finally, p_g, the gel pressure at the time-step *t,* can be assessed from:

$$p_g^a(t) = M_g \left\langle \frac{4}{3}\pi R_a^3 \cdot V_{gel}^{mol} \cdot s \cdot \zeta(t) - \varphi \frac{4}{3}\pi \left[(R_a + t_c)^3 - R_a^3 \right] \right\rangle \tag{6}$$

204 4. The pressure causes cracking of the aggregate and cement paste. Whatever the reactive
205 silica distribution in the aggregate, the propagation of cracks in small specimens containing
206 large aggregate can be rapid and can occur for low pressures, while the propagation is more
207 difficult for larger specimens containing smaller aggregates and needs higher pressure (Figure
208 5-d). In the framework of fracture mechanics [44-45], the maximal normal stress in the
209 vicinity of an inclusion (e.g. the aggregate) that induces pressure on a matrix (e.g. the cement
210 paste) is given by:

$$\sigma(r) = \frac{K_I}{\sqrt{2\pi r}} \tag{7}$$

With σ, the maximal normal stress at the point M located at distance r from the edge of the inclusion (Figure 5-d) and K_I, the stress intensity factor obtained for a specimen in stress-free conditions from the relation:

$$K_I = p_g^a \cdot f\left(\frac{R_a}{L}\right) \tag{8}$$

where f is a function increasing with the ratio R_a/L (which can be obtained in [41]), with R_a the aggregate radius and L the dimension of the specimen (a: superscript relative to the size of the reactive aggregate).

Smaller expansion in smaller specimen

The larger the aggregate size compared to the specimen size, the larger the normal stress at a given distance from the aggregate (Equations 7 and 8). Thus, the tensile strength at the boundary of the specimen can be reached for a smaller pressure (Figure 5-d) and cracks can be initiated earlier. Once concrete cracks, ASR-gels can be accommodated by cracking without creating supplementary pressure [46,47] and can even leach off through the porosity induced by cracking. Thus, the pressure in the gels falls, which stops the expansion.

If the pressure necessary to cause cracks is lower for small specimens containing large-sized aggregate, the pressure of the gel will fall sooner in the case of the 20x20x160-mm specimens containing the 1250-2500-µm aggregate than for the 70x70x280-mm specimens containing the same aggregate, and thus cause smaller expansion.

Pessimum effect or scale effect

The scale effect can also explain the pessimum effect of ASR expansion with aggregate size. For the largest aggregates, a part of the difference of expansion can be explained by a delay in the attack of the reactive silica by the hydroxyl ions due to the diffusion of the ions into the aggregate [23]. Measurements confirmed that the expansion rate was slower in the largest particles whatever the size of the specimens (Figure 3). However, even when the final value was reached, ASR expansion remained lower for the largest aggregates in the smallest

235 specimens. As explained above, the 20x20x160-mm specimens containing the 1250-2500-µm
236 aggregate were more affected by the scale effect than the specimens containing the 315-630-
237 µm aggregate: a larger aggregate induced a greater stress intensity factor (Equation 8).
238 Therefore, the part of reactive silica consumed when cracking appeared is lower when
239 cracking appears in the specimens containing the largest aggregate. Once cracking occurs, the
240 gel is accommodated by the cracks and the gel produced after cracking leads to little
241 supplementary pressure. Expansion ceases before the chemical reaction stops, giving a final
242 expansion lower than that for the largest aggregate. This is consistent with the experimental
243 determination of the degree of reaction performed with chemical attack [47] and SEM image
244 analysis [48]: expansion stopped while the degree of reaction was still increasing. The
245 pessimum effect versus specimen size is not an intrinsic phenomenon; it is due to the scale
246 effect, which depends on the 'specimen size to aggregate size' ratio. In this experimentation,
247 only mortars were tested and the pessimum effect disappeared for aggregate of 1.25-2.5 mm
248 when tests were performed in specimens of 70 mm. For concrete, the pessimum still exists for
249 aggregate of 4-8 mm in specimens of 70 mm [24]. If the scale effect (combination of the
250 aggregate size effect and the specimen size effect) is identical for concrete, specimens of more
251 than 250 mm could be necessary to remove the pessimum effect for such aggregates.
252 Supplementary investigations are necessary to analyse this effect on concrete.

253 ***Effect of the reactive silica content on the scale effect***

254 At last, it can also be used to analyse the effect of the reactive silica content on ASR
255 expansion (Figure 1). As shown in Figure 6, the final expansions measured on specimens
256 containing the different aggregates were not proportional to the reactive silica content.
257 Moreover, the specimens containing opal were much more damaged and cracked than those
258 with the other aggregates. This could have been due to the large concentration of reactive
259 silica contained in opal. A larger reactive silica content would induce a higher gel pressure

(Equation 6) and thus a greater stress intensity factor (Equation 8) for opal than for the siliceous limestone. Therefore, the ratio between the total reactive silica and the reactive silica consumed when cracking appeared was not the same. The part of reactive silica consumed would be lower when cracking appeared in the specimens containing opal than in the specimens containing the siliceous limestone. Once cracking had occurred, cracks accommodated the gel, and expansion stopped before the chemical reaction finished, without proportionality with the total reactive silica. This effect was probably very important in the case of specimens containing opal in which cracks were very large at the end of the experiment (Figure 2).

The concept of stress intensity factor appears to be important for an understanding of the development of ASR expansion in concrete. The larger the stress intensity factor K_I is, the faster cracks appear and the cracking could lead to reduction of the expansion through gel accommodation and exudation. The ratios between specimen and aggregate sizes were very high in these experiments. This shows that it could be difficult to use specimens large enough to avoid the scale effect. One possibility would be to try to control the aggregate and the specimen sizes so as to perform the test with similar stress intensity factors and thus to have similar cracking conditions as proposed in [42,43] but this would be difficult to do, particularly as far as controlling the aggregate size is concerned. Another possibility is to understand the scale effect through a model that can be used to analyse expansion tests. This is the aim of the modelling presented in the next part.

3. Modelling ASR expansion

The model used in this paper is an improvement on the microscopic model [34]. It was based on previous models [33, 35-37,39] and attempted to predict the damage and the expansion of a Representative Elementary Volume (REV) of concrete containing a mix of reactive

aggregates of different sizes. The reaction between the reactive silica and the alkali was determined through the mass balance equation, which describes the diffusion mechanism in the aggregate and the fixation of the alkali in the ASR gels. The mechanical part of the model is based on damage theory in order to assess the decrease of stiffness of the mortar due to cracking caused by ASR and to calculate the expansion of the REV [34]. Some modifications were made in this model: the threshold of alkalis was re-evaluated in accordance with the results present above and the combined effects of specimen and aggregate sizes and reactive silica content on expansions were taken into account.

3.1 Presentation of the model

3.1.1 Diffusion of alkali

The diffusion of ions in the aggregate partly controls the kinetics of the chemical attacks and of the expansion. At the beginning of ASR, hydroxyl ions attack the reactive silica of the aggregate. Hydroxyl ions come from the pore solution and thus the external boundary of the reactive aggregates is attacked first. If the reactive silica is uniformly distributed in the aggregate, the reactive silica closest to the pore solution is attacked first (Figure 5-a top). If the reactive silica occurs in veins, the penetration of hydroxyl ions is not uniform but veins in contact with the pore solution are attacked first (Figure 5-a bottom). Therefore, in both cases, the transport of ionic species in the aggregate can be modelled by an equivalent diffusion of ions from the pore solution to the aggregate core. The diffusion is not the only phenomenon which impacts the kinetics of ASR-expansion: the time necessary for the attack of the reactive silica by hydroxyl ions and for the formation of ASR-gels is taken into account through a depletion term in the mass balance equation [34]. This term models the alkali consumed by the ASR-gel formation. This alkali consumption is assumed to be linear with the alkali concentration in the aggregate. The temperature of storage for the experiment was 60°C. It accelerates ASR considerably compared to the environmental conditions of real damaged

309 structures and can affect the nature of the gel. It impacts the values of the kinetic parameters
310 but should not affect the principle of the modelling.
311 As in the previous model [34], only the diffusion of ions in the aggregate was considered
312 since the kinetics of diffusion in aggregates was much slower than in cement paste [35].
313 Therefore, the alkali concentration at the surface of aggregates was assumed to be equal to the
314 concentration of the NaOH solution. The kinetics of the expansion was thus partly controlled
315 by the diffusion in the aggregate, which is one of the kinetic parameters of the model. This
316 assumption is relevant for small specimens or when there is no chemical exchange with the
317 environment but it can be discussed for larger specimens immersed in NaOH solution. In the
318 experiments presented here, the largest specimens showed the slowest rate of ASR-expansion
319 (Figure 3). This can be explained by the diffusion of the alkali into the specimens. The initial
320 alkali concentration in the pore solution was sufficient to initiate the reaction. Alkalis were
321 quickly consumed by the ASR gel and supplementary alkalis were necessary to maintain gel
322 production. The alkali came from the solution and diffused into the mortar. Thus, more time
323 was necessary for alkali to reach the centres of the largest specimens than the centres of
324 smaller ones. Thus an alkali gradient appeared in the specimens. In consequence, at a given
325 time, a gradient of expansion existed between aggregates located close to the external
326 boundary and aggregates located in the core of the specimen. Only complete discretization of
327 the whole specimen [24,31,32] would allow this difference of expansion to be considered.
328 The aim of the modelling used in this paper was to evaluate the material behaviour that could
329 be represented by measurements performed on small specimens. Therefore, the phenomenon
330 of diffusion in the specimen was not taken into account. This modelling can give a good
331 representation of the expansion kinetics of concrete damaged by ASR measured on small
332 specimens (with width smaller than 40 mm, for which the effect of the alkali gradient is
333 negligible).

3.1.2 Threshold of alkali concentration

In the previous model, a threshold of alkali concentration of 0.625 mol/l of Na^+ was considered, under which ASR did not occur [34]. It was based on experimental data showing that, with an alkali content lower than 3 kg per m^3 of concrete, no ASR-expansion was observed [49-52]. In tests performed in non-saturated conditions (in air with RH above 95%), the concentration of alkali played an important role in the attack of the silica. In the present work, all the specimens were kept immersed in alkali solution and, thus, the alkali was supplied in abundant quantities. The experiments performed on specimens immersed in three alkali concentrations (0.77, 1 and 1.25 mol/l) showed negligible differences. Considering a threshold of 0.625 mol/l, the expansion of the mortars kept in 0.77 mol/l solution should be significantly slower than the expansion of the mortars kept in 1.25 mol/l solution. With this threshold, the alkali concentration in the aggregate has to be higher than 0.625 mol/l before the reactive silica is attacked. The gel production kinetics is then proportional to the difference between the alkali concentration in the paste and the threshold. The alkali concentration gradient between the paste and the aggregate remains too small to induce the same reaction speed as for the other concentrations. This is not in accordance with the expansion kinetics measured on specimens (Figure 1). Therefore, the gradient must be close for the three concentrations and consequently the alkali consumption by the silica must begin as soon as alkalis are present in the aggregate, without a threshold. The result of this assumption is shown in Figure 7: if no threshold is taken into account, the expansions determined by the modelling at 50 days are of the same order as the expansions obtained for the measurements. The apparent threshold effect observed in experimentations [49-52] can be explained by the alkali fixation in C-S-H. This fixation consumed a part of alkali which are no more available in the pore solution and reduced the attack kinetics and consequently the ASR-

358 expansion kinetics. All these phenomena can be explained without considering a threshold of
359 alkali concentration for the attack of the silica.

360 ***3.1.3 Effective ASR-gel***

361 The ASR expansion calculated by the model is imposed by the effective volume of ASR-gel.
362 The effective volume of gel is deduced from the total volume of gel, which is proportional to
363 the number of moles of ASR gel formed after the attack of the reactive silica (Equation 7).
364 Once cracking appears in the specimens, a part of the rest of the gel $<V^{gel} - V^{poro}>$ is
365 assumed to be accommodated by cracks created in the aggregate and in the cement paste by
366 the ASR-gel pressure. This gel accommodation by cracks stops the increase of the ASR-gel
367 pressure. This part depends on the scale effect: the larger the aggregate in comparison to the
368 specimen, the greater the volume of ASR gel accommodated. This phenomenon is also
369 affected by the reactive silica content of the aggregate. As explained in the analysis of the
370 experiments, the greater the reactive silica content is, the stronger is the non-linearity due to
371 cracking. Fracture mechanics concepts show that the aggregates closest to the external
372 boundary are the first to produce cracks. In order to quantify this effect, it can be assumed that
373 these aggregates lead to less pressure than the aggregates located in the core of the specimens.
374 As for the diffusion in cement paste, this will lead to a gradient of deformation between the
375 external boundary and the core and thus to internal stresses. The scale effect appears to be a
376 highly non-linear phenomenon. Therefore, an exponential function is proposed to model the
377 consequences on ASR expansions. An empirical relationship to quantify the reduction of the
378 gel amount effectively used to assess the pressure is thus assumed and applies equally to all
379 the aggregates of a given size i without consideration for their location compared to the
380 specimen boundary:

$$V_a^{eff} = \left\langle V_a^{gel} - V_a^{poro} \right\rangle^+ \times \max\left[\exp\left(-c \frac{2R_a}{L} s^x \right) \right] \quad (9)$$

With V_a^{eff}: the effective volume of gel, c: the scale effect fitting coefficient and χ: the silica content exponent.

The pressure imposed on the aggregate and thus on the cement paste depends on the effective volume of gel. Moreover, if the distribution of the reactive silica is uniform in the aggregate, the pressure will be isotropic (Figure 5-c). If the reactive silica is contained in veins in the aggregate, the large number of aggregate particles in the specimens means that the orientation of the veins in the specimens is randomly distributed and the mean resulting pressure can be considered as isotropic too (Figure 5-c). The effective volume of gel is then used in the mechanical model presented in [34] to deduce the resulting expansion.

3.2 Comparison with experiments

3.2.1 Parameters

Table 2 sums up the parameters used in the modelling, stating the symbols, the methods used for the identification, the values and the units. Three parameters (unique, independent of the other variables, and usable for all experiments and all aggregate types studied in this work) of the physicochemical modelling (thickness of the connected porous interface zone t_c, molar volume of ASR gel V_{gel}^{mol}, and scale effect fitting coefficient c – equations 4, 6 and 9) were obtained by curve fitting on the final expansions measured on the specimen of size 70 x 70 x 280 mm with the four different size classes (0-315, 315-630, 630-1250 and 1250-2500 µm) of siliceous limestone (SL – Figure 8). The parameters were first determined without considering the effect of the silica content exponent ($\chi = 0$) since the specimens involving the curve fitting contained the same aggregate. Once these three parameters had been assessed, the value of χ was determined by fitting the final expansion of mortars containing opal as aggregate (O – Figure 8). As explained above, the coefficient of alkali diffusion in aggregate, D_a, was used as a kinetic parameter. This coefficient can depend on the nature of the aggregate. It was obtained by curve fitting the results obtained on specimens of size 20 x 20 x

160 mm (Figure 9). The coefficients of diffusion in aggregate (D_a) thus obtained by curve fitting were respectively equal to 2.0 x 10^{-15}, 5.0 x 10^{-14}, 4.0 x 10^{-16} and 2.0 x 10^{-16} m^2/s for the siliceous limestone, opal, quartzite and quartz aggregate. It can be noted that the values were considerably lower than the usual value of diffusion coefficient determined for cement paste (about 10^{-12} m^2/s); the assumption of fast alkali supply at the surface of aggregate is thus verified. However, these values appear to be very small compared to coefficient of diffusion measured for quartzite [53]. It can be explained by the assumption used to determine the kinetics of the formation of ASR-gels. In this modelling, the kinetics was driven by two main phenomena: the diffusion of ions in the aggregates and the kinetics of the attack of reactive silica by alkali and hydroxyl [34]. The attack was assumed to be linear with the alkali concentration in the aggregate and only one parameter was used for all the aggregates. This parameter was fitted for siliceous limestone [34]. In the reality, the mechanisms leading to the gel formation are more complex and this simplified assumption can be responsible of the overestimation of the speed of the silica attack. It can lead to underestimation of the speed of diffusion. Improvements of the assumed kinetics of silica attack could lead to more realistic coefficients of diffusion for aggregates. However, this kinetics of silica attack could depend on the nature of the reactive silica and on the pH of the pore solution and several parameters could be necessary to obtain relevant results which could be very difficult to measure.

3.2.2 Calculations

Expansions obtained by modelling are compared with the measurements in Figures 9 and 10. Figure 9 shows the expansions obtained with 20 x 20 x 160-mm specimens containing two aggregate sizes (15% of 315-630 and 15% of 630-1250 µm) for the four natures of aggregate. Only the coefficient of diffusion and the silica content exponent were fitted on these results. The fitting concerning the final expansion of the siliceous limestone was only performed on the largest specimens (70x70x280 mm) and for specimens containing only aggregate of the

same size. Except for the kinetics of expansion obtained for specimens containing opal, both kinetics and final expansions obtained by the calculations were in accordance with the measurements for the four types of aggregate. The description of the expansion kinetics by the model is globally possible: presence of a latent time before initiation of the expansion, followed by a high rate of expansion and ending by a low rate to reach the final expansion.

Concerning the effect of the alkali concentration of the immersion solution, the difference between the final expansion predicted by the model (0.70%) and the mean measured expansion (0.65%) is lower than 10%. The calculation does not show any difference in final expansions between the three alkali concentrations: the model assumes that all the reactive silica is consumed in the three conditions and, thus, the volume of ASR gel created is the same, leading to the same ASR-expansion. The expansion rates obtained by the model at the beginning of expansion are in good agreement with experiments. This confirms that, in the case of specimens immersed in alkali solutions, no alkali threshold has to be considered (unlike for specimens exposed to a saturated environment [34]).

The curve obtained by the model for opal did not fit the experimental results well. At the beginning of the experiment, the slopes of the two curves were the same but, after about 50 days, the measurements showed a speeding-up of the expansions which was not obtained by the calculation. This can probably be attributed to crack opening for opal specimens as the specimens containing opal aggregate presented much larger cracks than specimens of the same size cast with the other aggregates. First, cracks opening increased the apparent expansion. These cracks could also cause a great increase in diffusion in the specimens, which could accelerate the reaction.

The comparison of the calculated final expansions obtained for the three specimen sizes (20 x 20 x 160 mm, 40 x 40 x 160 mm, 70 x 70 x 280 mm) and the four aggregate sizes of the siliceous limestone with the measurements is shown in Figures 10 and 11. Concerning these

values, only the measurements performed on the largest specimens were used for parameter identification. The calculated results for all the combinations are in good accordance with the measurements (Figure 10). The scale effect of ASR expansion pointed out in experimentations is rather well-predicted (Figure 11). The differences between calculated and measured expansions are lower than 15% except for the expansions obtained on the smallest specimens (20x20x160 mm) containing the largest aggregate (1250-2500 µm), where the difference is about 30% (Figure 10).

3.2.3 Discussion

The molar volume of ASR gel obtained by curve fitting in this work was about 170 cm^3/mol. It was higher than the molar volume obtained in the previous modelling performed for specimens kept in air at 95% relative humidity [34] and higher than the molar volume of C-S-H (about 100 cm^3/mol [54]). The differences can be explained by the conditions of conservation (in saturated air in [34] and immersed in NaOH solution in this work) which could have had a marked effect on the gel morphology and thus on the gels' capability to absorb water. The ASR gels were produced in pore solution with different water contents and alkali concentrations. The compositions of the gel were therefore different and thus the molar volume was different. Concerning the water, ASR gels formed in specimens kept in solution can absorb much more water than those in humid air (R.H. >95%).

The thickness of the connected porous interface zone (t_c equal to 14.0 µm) was also higher than that found in [34], which was about 1 µm. This value was determined to obtain the final expansions of four aggregate sizes while only two aggregate sizes were studied in the previous work. The molar volume of the gel was higher and therefore more connected porous volume was necessary to accommodate the gel. The ASR gels could permeate over a long distance because the molar volume was high and because the viscosity was small due to high water and alkali contents. This value is in accordance with the results found in the literature

[55-56] showing that the interfacial transition zone between aggregate and cement paste can reach 20 µm.

4. Conclusion

This paper has aimed to investigate and quantify the combined effects of aggregate and specimen sizes on ASR expansion and the influence of the reactive silica content of aggregate on this effect. In order to quantify these effects on ASR expansion, a microscopic model was improved. The main conclusions can be summarized as follows:

1. A scale effect, combining the effects of aggregate size, reactive silica content and specimen size on ASR expansion, has been highlighted by experimentation. A temporary pessimum size effect had previously been shown to exist due to the speed of the attack of the reactive silica on the aggregate: the larger the aggregate, the slower the penetration of ions into the aggregate and thus the slower the expansion [23]. In this paper, only stabilized expansions were compared, which pointed out another pessimum effect. The pessimum size effect of stabilized expansion appears not to be an intrinsic phenomenon of ASR expansion but to depend on the size of the specimen used to perform the expansion test. For the largest specimens, no pessimum effect was detected for the aggregate size used in this study. The scale effect has been explained by fracture mechanics concepts: the larger the ratio between the aggregate and specimen sizes, the larger the stress intensity factor around the aggregate and the faster the cracking around the aggregate. After cracking, a part of the ASR gels can be accommodated by cracks.
2. Considering that the scale effect is unavoidable for experimental specimens (the ratio between specimen and aggregate sizes should be larger than 100 to significantly decrease the effect), the results of expansion tests should be analysed with respect to

505 this effect. The modelling proposed took the scale effect into account through an
506 empirical relationship considering underlying linear fracture mechanics concepts.
507 Calculations are in good accordance with experiments for expansion tests performed
508 with ratios higher than 10 between specimen and aggregate sizes for the four
509 aggregates studied.

510 Finally, this paper points out the complexity of ASR expansion and states the numerous
511 parameters that have to be taken into account to obtain relevant calculations. Another
512 important conclusion is that stress-free expansions obtained on specimens cannot be directly
513 used as input parameters in structural models because they are strongly dependent on the
514 specimen size and on the conservation conditions during the expansion test. To be used,
515 stress-free expansion test results should be interpreted by considering the phenomena pointed
516 out in this work. Such an approach is possible: free expansion tests can be carried out to
517 assess the AAR advancement in aggregates, while the expansion in the conditions of the
518 damaged structures is assessed through a finite element inverse analysis able to combine the
519 fitting of the expansion measured on structures with the chemical advancement kinetics
520 deduced from laboratory tests [57].

521 Acknowledgements

522 The authors are grateful to Pr Eric Garcia-Diaz, Pr Benoît Fournier, Pr William Prince, Mr
523 Eric Bourdarot and Mr Etienne Grimal for their advice and suggestions, which have helped to
524 improve the analysis and the modelling.

525 References

526 [1] S. Dent Glasser, N. Kataoka, The chemistry of alkali-aggregate reaction, Cement and
527 Concrete Research, 11 (1) (1981) 1-9.
528 [2] R. Dron, F. Brivot, Thermodynamic and kinetic approach to the alkali-silica reaction.
529 Part 2: Experiment, Cement and Concrete Research, 23 (1) (1993) 93-103.
530 [3] T. Ichikawa, M. Miura, Modified model of alkali-silica reaction Cement and Concrete
531 Research, 37 (9) (2007) 1291-1297.
532 [4] T. Ichikawa, Alkali-silica reaction, pessimum effects and pozzolanic effect, Cement
533 and Concrete Research, 39(8) (2009) 716-726.

[5] D. McConnell, R.C. Mielenz, W. Y. Holland, K.T. Greene, Cement-aggregate reaction in concrete, Journal of the American Concrete Institute, Proceedings Vol.44, No.2, October 1947, pp.93-128.
[6] T.M. Kelly, L. Schuman, F.B. Hornibrook, A study of alkali-silica reactivity by means of mortar bar expansions, Journal of the American Concrete Institute, Proceedings Vol.45, No.1, September 1948, pp.57-80.
[7] S. Diamond, N. Thaulow, A study of expansion due to alkali-silica reaction as conditioned by the grain size of the reactive aggregate, Cement and Concrete Research,4 (4) (1974) 591-607.
[8] S. Sprung, Influence of the alkali-aggregate reaction in concrete, Symposium on Alkali-Aggregate Reaction – Preventive Measures, Icelandic Building Research Institute and State Cement Works, Reykjavik, Iceland, 1975, pp.231-244.
[9] D. W. Hobbs, W. Gutteridge, Particle size of aggregate and its influence upon the expansion caused by the alkali-silica reaction, Magazine of Concrete research, 31 (109) (1979) 235-242.
[10] D. Lenzner, U. Ludwig, Alkali aggregate reaction with opaline sandstone, 7th International Congress on the Chemistry of Cement, Septima (Ed.), Paris, France, 1980, Vol.3, pp.VII-119 - VII-123.
[11] M. Kawamura, K. Takemoto, S. Hasaba, Application of quantitative EDXA analyses and microhardness measurements to the study of alkali-silica reaction mechanisms, 6th International Conference of Alkalis in Concrete, Idorn G.M. and Rostam S. (Editors), Copenhagen, Denmark, 1983, pp.167-174.
[12] G. Baronio, M. Berra, L. Montanaro, A. Delmastro, A. Bacchiorini, Couplage d'action de certains paramètres physiques sur le développement de la réaction alcalis-granulats, From Materials Science to Construction Materials Engineering, 1st International RILEM Congress on Durability of Construction Materials, Versailles, France, 1987, Vol.3, pp 919-926.
[13] X. Zhang, G. W. Groves, The alkali-silica reaction in OPC-silica glass mortar with particular reference to pessimum effects, Advances in Cement Research 3 (9) (1990) 9-13.
[14] C. Zhang, A. Wang, M. Tang, B. Wu, N. Zhang, Influence of aggregate size and aggregate size grading on ASR expansion, Cement and Concrete Research, 29 (9) (1999) 1393-1396.
[15] A. Shayan, Value-added Utilisation of Waste Glass in Concrete, IABSE Symposium Melbourne 2002.
[16] Z. Xie, W. Xiang, Y. Xi, ASR Potentials of Glass Aggregates in Water-Glass Activated Fly Ash and Portland Cement Mortars, Journal of Materials in Civil Engineering,15 (1) (2003) 67-74.
[17] T. Kuroda, S. Nishibayashi, S. Inoue, A. Yoshino, Effects of the particle size of reactive fine aggregate and accelerated test conditions on ASR expansion of mortar bar, Transactions of the Japan Concrete Institute, 22 (2000) 113-118.
[18] Y. Shao, T. Lefort, S. Moras, D. Rodriguez, Studies on concrete containing ground waste glass, Cement and Concrete Research, 30 (1) (2000) 91-100.
[19] T. Kuroda, S. Inoue, A. Yoshino, S. Nishibayashi, Effects of particle size, grading and content of reactive aggregate on ASR expansion of mortars subjected to autoclave method, 12th International Conference on Alkali-Aggregate Reaction in Concrete, Tang M. and Deng M. (Editors), Beijing, China, 2004, pp.736-743.
[20] K. Ramyar, A. Topal, O. Andic, Effects of aggregate size and angularity on alkali–silica reaction, Cement and Concrete Research, 35 (2005) 2165-2169.
[21] M. Moisson, M. Cyr, E. Ringot, A. Carles-Gibergues, Efficiency of reactive aggregate powder in controlling the expansion of concrete affected by alkali-silica reaction (ASR), 12th

International Conference on Alkali-Aggregate Reaction in Concrete, Tang M. and Deng M. (Editors), Beijing, China, 2004, pp.617-624.
[22] S. Multon, M. Cyr, A. Sellier, N. Leklou, L. Petit, Coupled effects of aggregate size and alkali content on ASR expansion, Cement and Concrete Research, 38 (2008) 350-359.
[23] S. Multon, M. Cyr, A. Sellier, P. Diederich, L. Petit, Effect of aggregate size and alkali content on ASR expansion, Cement and Concrete Research, 40 (2010) 508–516.
[24] C.F. Dunant, K.L. Scrivener, Effects of aggregate size on alkali–silica-reaction induced expansion, Cement and Concrete Research 42 (6) (2012) 745–751.
[25] RFM Bakker, The influence of test specimen dimensions on the expansion of reactive alkali aggregate in concrete. Proceedings of the 6th ICAAR, Copenhagen, Denmark, 1983, pp. 369-375.
[26] C. Zhang, A. Wang, M. Tang, N. Zhang, Influence of dimension of test specimen on alkali aggregate reactive expansion, ACI Materials Journal, 96 (1999) 204-207.
[27] J. Duchesne, M-A. Bérubé, Effect of the cement chemistry and the sample size on ASR expansion of concrete exposed to salt, Cement and Concrete Research, 33 (2003) 629–634.
[28] N. Smaoui, M-A. Bérubé, B. Fournier, B. Bissonnette, Influence of specimen geometry, direction of casting, and mode of concrete consolidation on expansion due to ASR. Cement, Concrete and Aggregate, 26 (2004) 58-70.
[29] P. Goltermann, Mechanical predictions on concrete deterioration. part 1: Eigenstresses in concrete, ACI Materials Journal, 91 (6) (1994) 543–550.
[30] Z.P Bazant, A. Steffens, Mathematical model for kinetics of alkali-silica reaction in concrete, Cement and Concrete Research, 30 (2000) 419–428.
[31] I. Comby-Perot, F. Bernard, P.-O. Bouchard, F. Bay, E. Garcia-Diaz, Development and validation of a 3D computational tool to describe concrete behaviour at mesoscale. Application to the alkali-silica reaction, Computational Material Science, 46 (4) (2009) 1163-1177.
[32] C.F. Dunant, K.L. Scrivener, Micro-mechanical modelling of alkali–silica-reaction induced degradation using the AMIE framework, Cement and Concrete Research 40 (4) (2010) 517–525.
[33] Y. Furusawa, H. Ohga, T. Uomoto, An analytical study concerning prediction of concrete expansion due to alkali-silica reaction, in Malhotra (ed.), 3rd International Conference on Durability of Concrete, Nice, France, 1994, pp 757–780.
[34] S. Multon, A. Sellier, M. Cyr, Chemo–mechanical modeling for prediction of alkali silica reaction (ASR) expansion, Cement and Concrete Research, 39 (2009) 490-500.
[35] S. Poyet, A. Sellier, B. Capra, G. Foray, J.-M. Torrenti, H. Cognon, E. Bourdarot, Chemical modelling of Alkali Silica reaction: Influence of the reactive aggregate size distribution, Materials and Structures, 40 (2007) 229–239.
[36] A. Nielsen, F. Gottfredsen, F. Thogersen, Development of stresses in concrete structures with alkali-silica reactions, Material and Structures, 26 (1993) 152-158.
[37] A. Sellier, J-P. Bournazel, A. Mébarki, Modelling the alkali aggregate reaction within a probabilistic frame-work, 10th International Conference of Alkali Aggregate Reaction, Melbourne, Australia, 1996, pp 694-701.
[38] A. Suwito, W. Jin, Y. Xi, C. Meyer, A mathematical model for the pessimum effect of ASR in concrete, Concrete Science and Engineering, 4 (2002) 23-34.
[39] A. Sellier, J-P. Bournazel, A. Mébarki, Une modélisation de l'alcali-réaction intégrant une description des phénomènes aléatoires locaux, Materials and Structures 28 (1995) 373-383.
[40] L. Charpin, A. Ehrlacher, A computational linear elastic fracture mechanics-based model for alkali–silica reaction, Cement and Concrete Research, 42 (4) (2012) 613-625.

633 [41] H.W. Reinhardt, O. Mielich, A fracture mechanics approach to the crack formation in
634 alkali-sensitive grains, Cement and Concrete Research, 41 (3) (2011) 255-262.
635 [42] X.X. Gao, S. Multon, M. Cyr, A. Sellier, Optimising an expansion test for the
636 assessment of alkali-silica reaction in concrete structures, Materials and Structures**,** 44 (2011)
637 1641–1653.
638 [43] X.X. Gao, Contribution to the requalification of Alkali Silica Reaction (ASR)
639 damaged structures: Assessment of the ASR advancement in aggregates, PhD thesis, 2010,
640 Université de Toulouse, France.
641 [44] J. Lemaître, J-L. Chaboche, Mécanique des Matériaux Solides, Dunod (Eds.), Paris,
642 France, 1988.
643 [45] D. François, A. Pineau, A. Zaoui, Comportement mécanique des matériaux :
644 viscoplasticité, endommagement, mécanique de la rupture, mécanique du contact, Hermes
645 Eds, 1993.
646 [46] V. Saouma, L. Perotti, Constitutive model for alkali-aggregate reactions, ACI
647 Materials Journal, 103 (3) (2006) 194-202.
648 [47] E. Garcia-Diaz, J. Riche, D. Bulteel, C. Vernet, Mechanism of damage for the alkali–
649 silica reaction, Cement and Concrete Research, 36 (2006) 395 – 400.
650 [48] M. Ben Haha, E. Gallucci, A. Guidoum, K.L. Scrivener, Relation of expansion due to
651 alkali silica reaction to the degree of reaction measured by SEM image analysis, Cement and
652 Concrete Research 37 (2007) 1206–1214.
653 [49] D.W. Hobbs, Deleterious alkali–silica reactivity in the laboratory and under field
654 conditions, Magazine of Concrete Research 45 (163) (1993) 103–112.
655 [50] C. A. Rogers, R. D. Hooton, Reduction in Mortar and Concrete Expansion with
656 Reactive Aggregates Due To Alkali Leaching, Cement, Concrete and Aggregates 13(1) (1991)
657 42-49.
658 [51] M.H. Shehata, M.D.A. Thomas, The effect of fly ash composition on the expansion of
659 concrete due to alkali–silica reaction, Cement and Concrete Research 30 (7) (2000) 1063–
660 1072.
661 [52] M.D.A. Thomas, B.Q. Blackwell, P.J. Nixon, Estimating the alkali contribution from fly
662 ash to expansion due to alkali-aggregate reaction in concrete, Magazine of Concrete Research
663 48 (177) (1996) 251–264.
664 [53] S. Goto, D. M. Roy, Diffusion of ions through hardened cement pastes Cement and
665 Concrete Research, 11 (5–6) (1981) 751-757.
666 [54] H.F.W. Taylor, Cement Chemistry, Academic Press, London, 1990.
667 [55] K. L. Scrivener, K. M. Nemati, The percolation of pore space in the cement
668 paste/aggregate interfacial zone of concrete, Cement and Concrete Research 26(1) (1996) 35-
669 40.
670 [56] K. L. Scrivener, A. K. Crumbie, P. Laugesen, The interfacial transition zone (ITZ)
671 between cement paste and aggregate in concrete, Interface science 12 (2004) 411-421.
672 [57] A. Sellier, E. Bourdarot E., S. Multon, M. Cyr, E. Grimal, Combination of structural
673 monitoring and laboratory tests for the assessment of AAR-swelling: application to a gate
674 structure dam, ACI Materials Journal 106 (3) (2009) 281-290.
675
676

677

678 TABLES

679
680
681

Table 1: Reactive silica contents of different aggregates [43]

Reactive silica (SiO_2)	*SL*	*O*	*Q*	*QA*
Percentage by mass (%)	6.9	50.4	7.6	2.7
Content (mol/m³ of aggregate)	3000	21900	3300	1170

682

683

Table 2: Parameters of model

Parameter	**Symbol**	**Identification**	**Value**	**Units**
Aggregate				
Reactive silica content	s	measurement	D.N.A.*	mol/m³
Coefficient of diffusion	D_a	curve fitting	D.N.A.*	m²/s
Porosity	p	usual value	0.01	%
Paste				
Porosity of mortar	p_{mort}	measurement	18.0	%
Thickness of the connected porous interface zone	t_c	curve fitting	14.0×10^{-6}	m
Gel				
Molar volume of ASR gel	V_{gel}^{mol}	curve fitting	1.7×10^{-4}	m³/mol
Scale effect coefficient	c	curve fitting	0.037	$(mol/m^3)^{-\chi}$
Silica content exponent	χ	curve fitting	0.75	-

684 * depends on the nature of the aggregate
685

686

687 # FIGURES

688

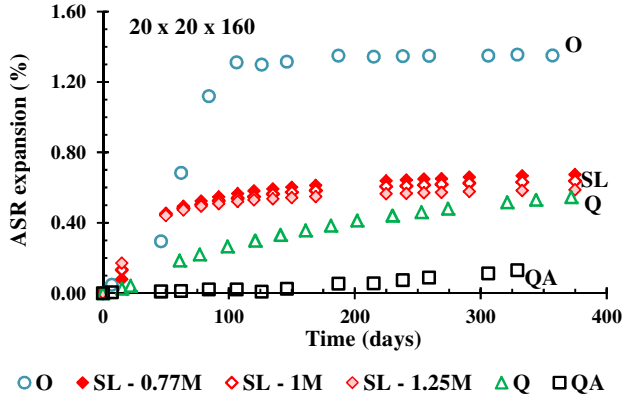

Figure 1: ASR expansions according to the alkali concentration of the immersion solution for SL (0.77, 1.0 and 1.25 mol/l) and to the nature of the aggregate (O: opal, SL: siliceous limestone, Q: quartzite and QA: quartz aggregate) stored in the 1 mol/l NaOH immersion solution

689

690

(a)

(b)

Figure 2: Cracking patterns of specimens cast with the siliceous limestone (a) and with opal (b)

691

692

693

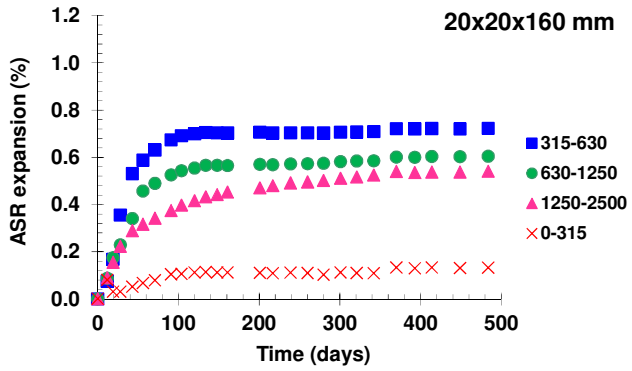

(a)

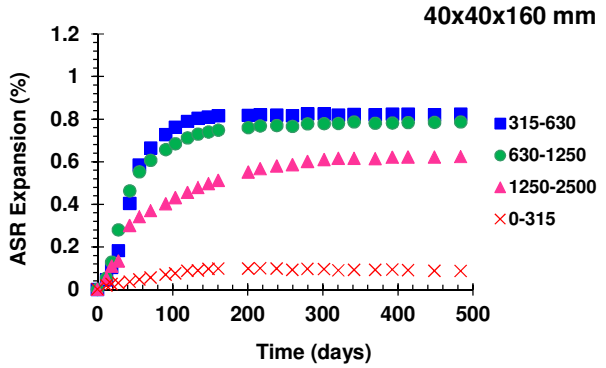

(b)

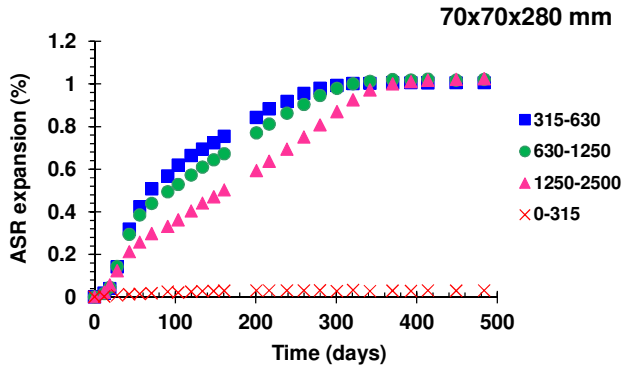

(c)

Figure 3: ASR expansions on prismatic specimens 20x20x160 mm (a), 40x40x160 mm (b) and 70x70x280 mm (c)

694

695

696

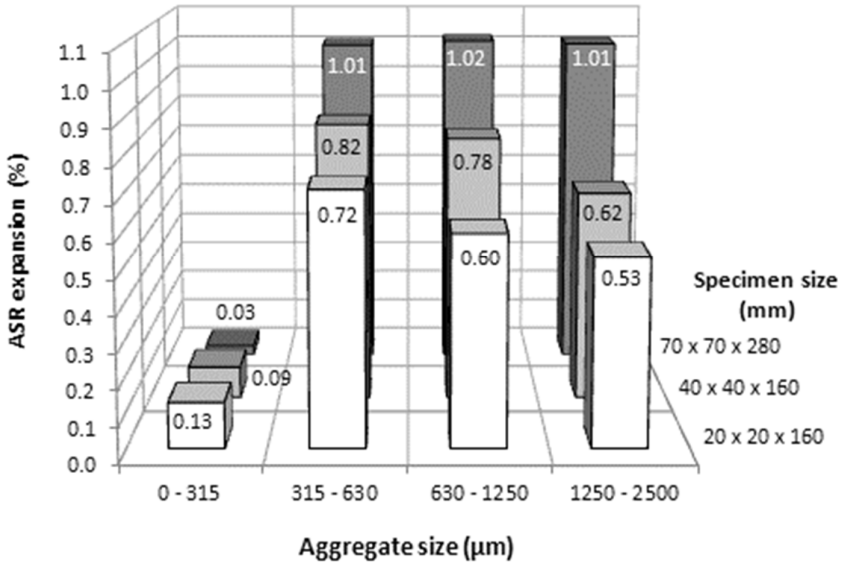

Figure 4: Final ASR expansions according to specimens size and aggregates size

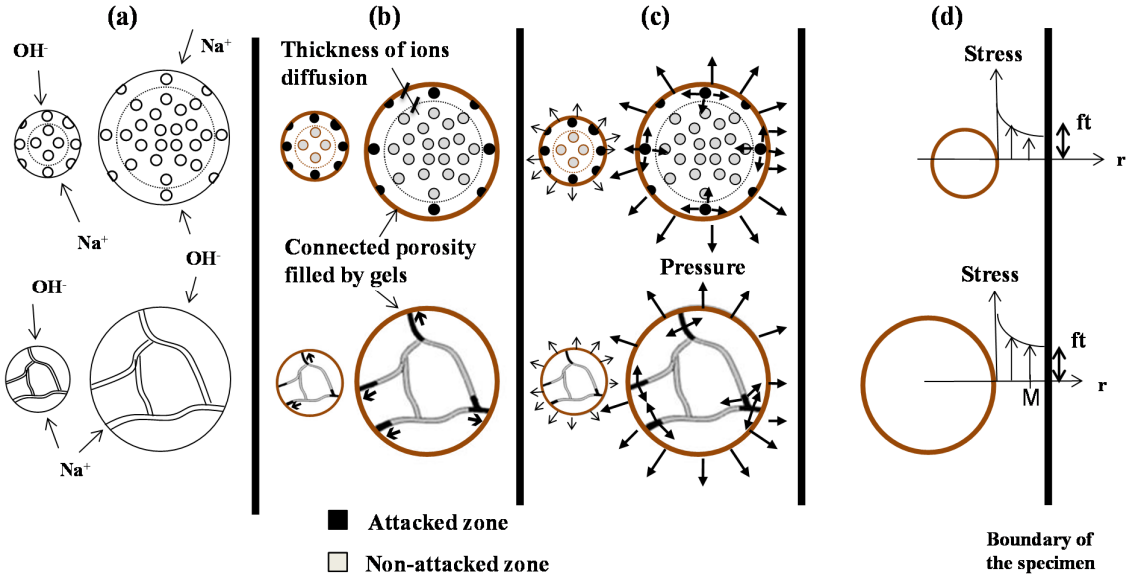

Figure 5: Four phases of ASR development: ion diffusion (a), reaction with the reactive silica (b), gel pressure (c), and stress development (d). Top line: diffuse reactive silica distribution, bottom line: veins

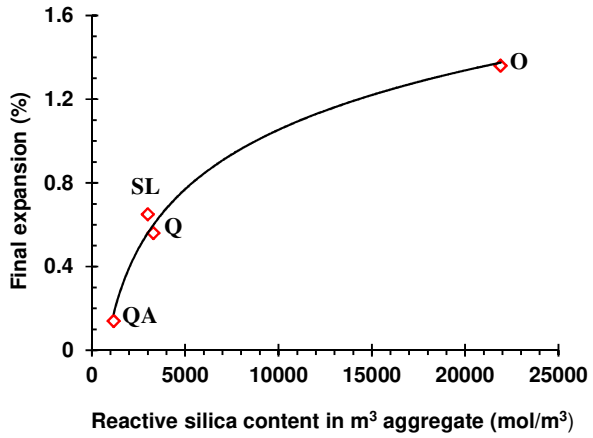

Figure 6: Final expansions according to reactive silica content

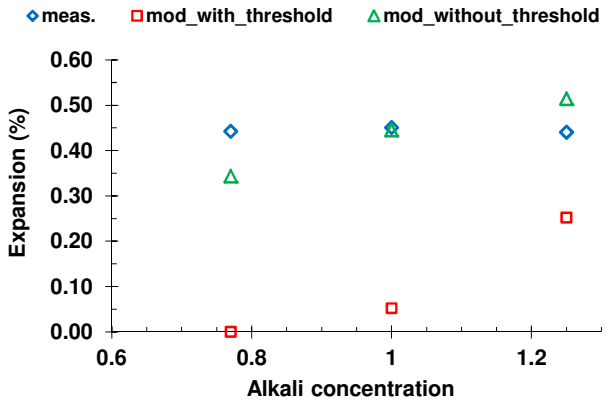

Figure 7: Measured and calculated expansions at 50 days according to the alkali concentration of the solution (calculations performed with or without the threshold of 0.625 mol/l)

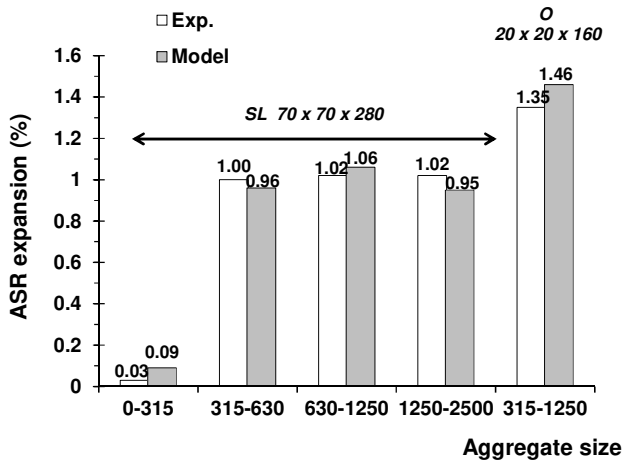

Figure 8: Identification of the modelling parameters

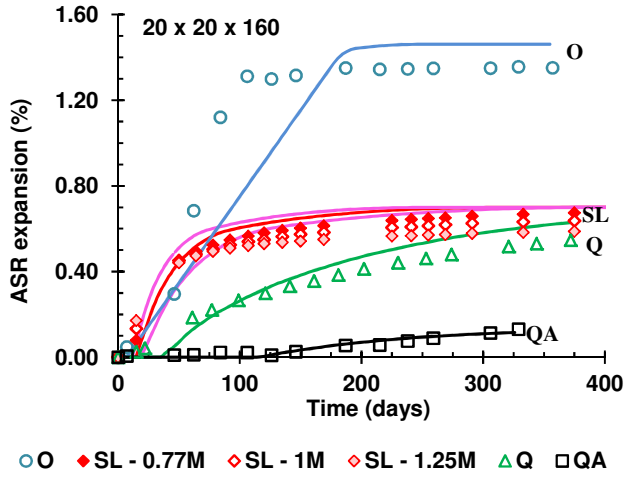

Figure 9: Comparison of calculated and measured expansions according to the alkali concentration of the immersion solution (0.77, 1.0 and 1.25 mol/l) and to the nature of the aggregate (O: opal, SL: siliceous limestone, Q: quartzite and QA: quartz aggregate)

707
708

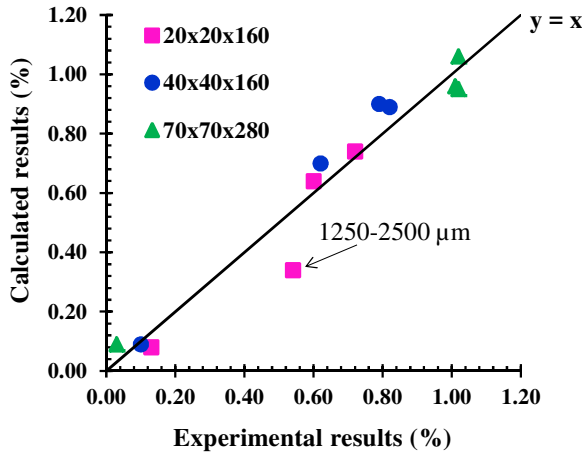

709
710 **Figure 10:** Comparison of calculated and measured final expansions for all the combinations
711 between the sizes of aggregates and specimens with siliceous limestone
712
713
714
715

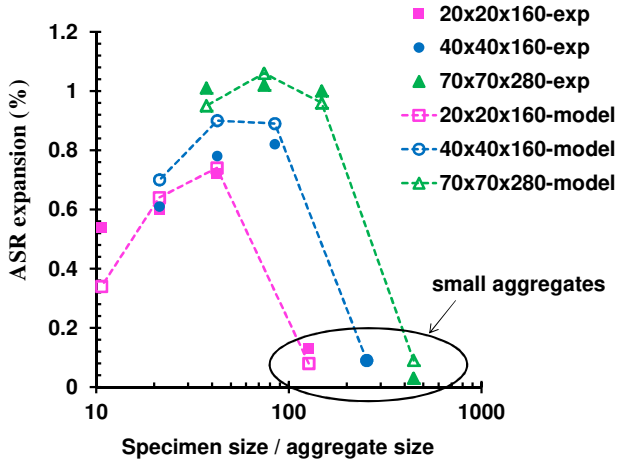

716
717 **Figure 11:** Scale effect of ASR expansion: experimental and modelling results
718
719